









# Therapy for Argentine hemorrhagic fever in nonhuman primates with a humanized monoclonal antibody

Larry Zeitlin<sup>a,1</sup> , Robert W. Cross<sup>b,c</sup>, Joan B. Geisbert<sup>b,c</sup>, Viktoriya Borisevich<sup>b,c</sup>, Krystle N. Agans<sup>b,c</sup> , Abhishek N. Prasad<sup>b,c</sup> , Sven Enterlein<sup>d</sup> , M. Javad Aman<sup>d</sup> , Zachary A. Bornholdt<sup>a</sup>, Miles B. Brennan<sup>a</sup>, Lioudmila Campbell<sup>a</sup>, Do Kim<sup>a</sup>, Neil Mlakar<sup>a</sup>, Crystal L. Moyer<sup>a</sup>, Michael H. Pauly<sup>a</sup>, William Shestowsky<sup>a</sup>, Kevin J. Whaley<sup>a</sup> , Karla A. Fenton<sup>b,c</sup>, and Thomas W. Geisbert<sup>b,c</sup>

<sup>a</sup>Mapp Biopharmaceutical, Inc., San Diego, CA 92121; <sup>b</sup>Galveston National Laboratory, University of Texas Medical Branch, Galveston, TX 77555; <sup>c</sup>Department of Microbiology and Immunology, University of Texas Medical Branch, Galveston, TX 77555; and <sup>d</sup>Integrated BioTherapeutics, Inc., Gaithersburg, MD 20878

Edited by Peter Palese, Icahn School of Medicine at Mount Sinai, New York, NY, and approved January 31, 2021 (received for review November 9, 2020)

The COVID-19 pandemic has reemphasized the need to identify safe and scalable therapeutics to slow or reverse symptoms of disease caused by newly emerging and reemerging viral pathogens. Recent clinical successes of monoclonal antibodies (mAbs) in therapy for viral infections demonstrate that mAbs offer a solution for these emerging biothreats. We have explored this with respect to Junin virus (JUNV), an arenavirus classified as a category A high-priority agent and the causative agent of Argentine hemorrhagic fever (AHF). There are currently no Food and Drug Administration-approved drugs available for preventing or treating AHF, although immune plasma from convalescent patients is used routinely to treat active infections. However, immune plasma is severely limited in quantity, highly variable in quality, and poses significant safety risks including the transmission of transfusion-borne diseases. mAbs offer a highly specific and consistently potent alternative to immune plasma that can be manufactured at large scale. We previously described a chimeric mAb, cJ199, that provided protection in a guinea pig model of AHF. To adapt this mAb to a format more suitable for clinical use, we humanized the mAb (hu199) and evaluated it in a cynomolgus monkey model of AHF with two JUNV isolates, Romero and Espindola. While untreated control animals experienced 100% lethality, all animals treated with hu199 at 6 d postinoculation (dpi) survived, and 50% of animals treated at 8 dpi survived. mAbs like hu199 may offer a safer, scalable, and more reproducible alternative to immune plasma for rare viral diseases that have epidemic potential.

Junin | monoclonal | therapy | hemorrhagic fever

Junin virus (JUNV), an arenavirus, is the causative agent of Argentine hemorrhagic fever (AHF). Although AHF is currently confined to Argentina, its geographical distribution has expanded since its discovery in 1958. As an endemic virus spread by exposure to the excreta of native ineradicable rodent populations, JUNV may be acquired during natural outbreaks for bioterror purposes (1) and indeed has been shown to be infectious by the aerosol route (2). Furthermore, the geographic range may continue to expand. Although uncommon, person-to-person transmission has been documented (3). The slow onset of AHF with nonspecific symptoms that may delay diagnosis, coupled with a debilitating hemorrhagic phase, make JUNV a threat to public health (4, 5). While an unlicensed attenuated vaccine manufactured in Argentina (6, 7) is used in high-risk individuals and reduces the incidence of AHF, the vaccine is in short supply, and 10 to 15 cases per year continue to be observed. Untreated, AHF has a mortality rate of 20% to 30%; however, treatment with immune plasma within 8 d of symptoms reduces the mortality rate to 1% (8, 9). Although highly effective, immune plasma has limitations (10); its potency varies from donor to donor, supplies are limited, and the use of immune plasma poses safety risks (e.g., transfusion-borne disease). Monoclonal antibodies (mAbs) offer a highly specific, potent, and generally safe—especially for nonhuman

antigen targets—antiviral drug platform that may provide an alternative to immune plasma in AHF patients.

We previously described a mouse-human chimeric anti-JUNV glycoprotein mAb, cJ199, derived from murine mAb GB-03-BE08 (11), that is a potent neutralizer in vitro and highly protective in a guinea pig model of AHF (12) when treatment was initiated as late as 7 d postinoculation (dpi). Here we report on efforts to further develop this mAb therapy for potential clinical use. Toward this goal, we generated a humanized version of cJ199 (hu199) and subsequently evaluated its therapeutic efficacy in guinea pigs and in nonhuman primates (NHPs) infected with one of two medically relevant strains of JUNV, Espindola or Romero.

## Results

**Humanization of J199.** Humanization of the originator murine J199 mAb was performed by traditional techniques (13). Hu199 and cJ199 were compared in a plaque neutralization assay using the Candid #1 strain. As Fig. 1A illustrates, the two mAbs had similar high neutralization potency (PRN<sub>50</sub>, 18 ng/mL and 21 ng/mL, respectively), indicating that the humanization process did not detectably impact mAb functionality.

## Significance

Despite the relatively high disease burden of arenaviruses in South America and Africa, there are currently no Food and Drug Administration-approved drugs for use in preventing or treating any arenavirus infection. Currently, the sole clinically validated treatment option for Argentine hemorrhagic fever (AHF), caused by Junin virus (JUNV), is administration of immune plasma. While the relative success associated with this treatment supports passive immunotherapy interventions, the recent expansion of mAbs used in a clinical setting for infectious diseases offer a highly specific, consistently potent, and generally safe alternative to immune plasma. Here we show that a humanized mAb is highly efficacious in guinea pig and nonhuman primate models of AHF.

Author contributions: L.Z. and T.W.G. designed research; R.W.C., J.B.G., V.B., K.N.A., S.E., M.J.A., Z.A.B., M.B.B., L.C., D.K., N.M., C.L.M., M.H.P., W.S., K.J.W., K.A.F., and T.W.G. performed research; L.Z., R.W.C., J.B.G., V.B., K.N.A., A.N.P., S.E., M.J.A., Z.A.B., M.B.B., L.C., D.K., N.M., C.L.M., M.H.P., W.S., K.J.W., K.A.F., and T.W.G. analyzed data; and L.Z., R.W.C., A.N.P., Z.A.B., C.L.M., K.A.F., and T.W.G. wrote the paper.

Competing interest statement: K.J.W. and L.Z. are co-owners of Mapp Biopharmaceutical, Inc., and Z.A.B., L.C., D.K., N.M., and C.L.M. are employees of Mapp.

This article is a PNAS Direct Submission.

This open access article is distributed under Creative Commons Attribution-NonCommercial-NoDerivatives License 4.0 (CC BY-NC-ND).

<sup>1</sup>To whom correspondence may be addressed. Email: larry.zeitlin@mappbio.com.

This article contains supporting information online at <https://www.pnas.org/lookup/suppl/doi:10.1073/pnas.2023332118/-DCSupplemental>.

Published March 8, 2021.

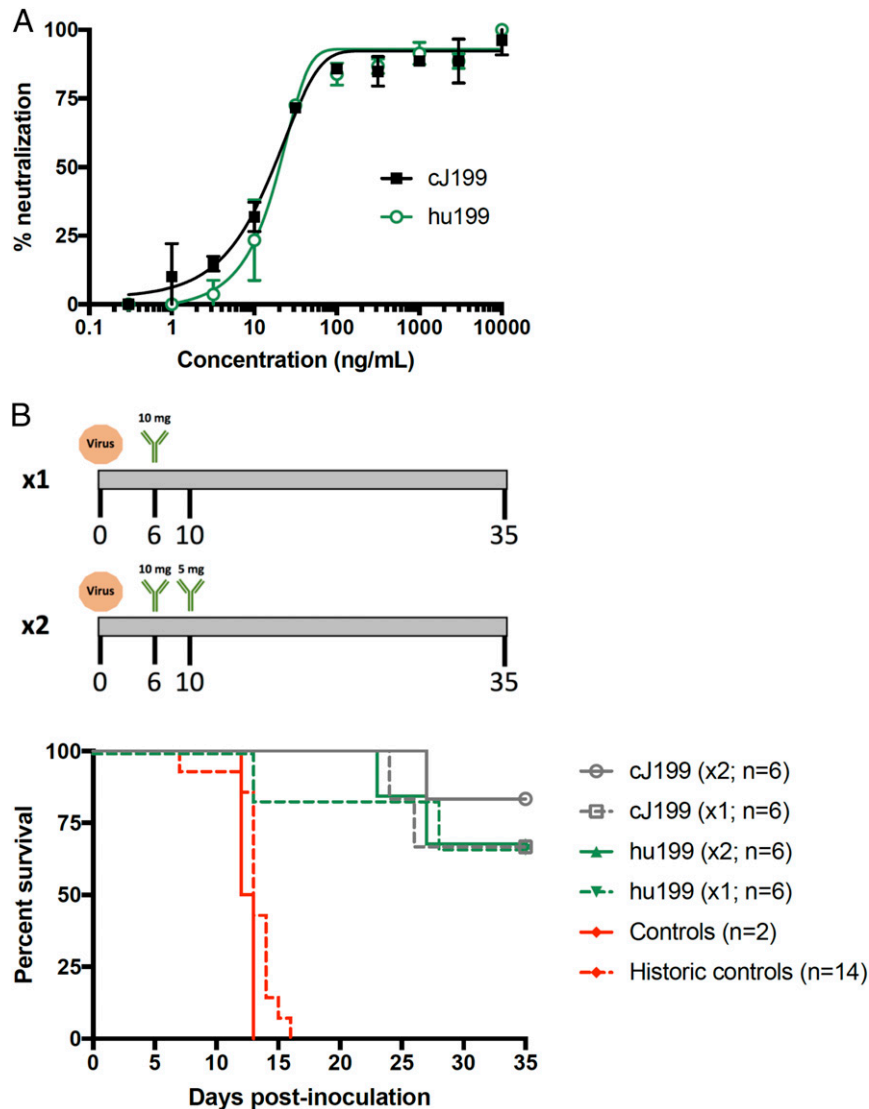


**Fig. 1.** Comparison of the chimeric mAb cJ199 and the humanized version hu199. (A). Neutralization activity as assessed using a plaque reduction assay with strain Candid #1. The percent inhibition of viral infection is displayed on the y-axis. Plotted points are the average of two replicates, with error bars denoting SD. (B) Protective efficacy in guinea pigs challenged with JUNV (Romero). (Upper) The experimental timeline for challenge and treatment with either cJ199 or hu199. Groups of animals ( $n = 6$  per treatment group;  $n = 2$  for the control group) were inoculated i.p. with virus (1,000 PFU) and treated with either a single dose i.p. (10 mg at 6 dpi; "x1") or two doses (10 mg at 6 dpi and 5 mg at 10 dpi; "x2"). (Lower) Survival curves showing statistically significant ( $P < 0.05$ , log-rank test) protective efficacy in all treated groups compared with untreated controls.

**Efficacy of hu199 in the Guinea Pig Model.** To confirm that in vivo efficacy was not impacted by humanization, hu199 and the chimeric version of the originator mAb, cJ199, were produced in *Nicotiana benthamiana* and compared in a guinea pig model of AHF. Groups of outbred guinea pigs were administered an intraperitoneal (i.p.) challenge with 1,000 PFU JUNV (Romero). Treatment groups received either a single 10 mg i.p. dose of mAb at 6 days postinoculation (dpi) or a 10 mg dose at 6 dpi and a subsequent 5 mg dose at 10 dpi. As Fig. 1B illustrates, control animals ( $n = 2$ ) experienced 100% lethality, with a mean time to death (MTD) of 13 d, identical to that of the historical control group ( $n = 14$ ; animals inoculated with the same viral stock and 1,000 PFU challenge). In contrast, animals treated with either cJ199 or hu199 experienced a significant ( $P < 0.05$ , log-rank test) survival benefit (67% and 83%, respectively). No obvious differences were observed between the chimeric and humanized mAb groups or between groups receiving one or two doses.

**Efficacy of hu199 in Nonhuman Primates.** Hu199 was next produced in CHOK1-AF cells that yield mAb with *N*-glycosylation profiles similar to the *N. benthamiana* expression system, with GnGn as the major *N*-glycan (> 75%) and the absence of fucosylated *N*-glycans (12, 14). This mAb was evaluated in a pilot study using a nonhuman primate (NHP) model of AHF. Briefly, animals were inoculated intravenously (i.v.) with 5,000 PFU of the Romero JUNV strain and treated i.v. with hu199 (50 mg/kg) at 5 dpi ( $n = 1$ ), 5 + 8 dpi ( $n = 2$ ), or 8 dpi ( $n = 1$ ). All treated animals survived for the duration of the study (SI Appendix, Fig. S1A). Historical controls ( $n = 2$ ) that received the same inoculum succumbed on day 13 and day 21 of the study. All animals were viremic on day 5 prior to the day 5 treatments ( $2.4 \pm 0.5 \log_{10}$  PFU/mL) (SI Appendix, Fig. S1B) and also exhibited some changes in hematology and serum biochemistry values (SI Appendix, Table S1). The animal treated on day 8 only, Pilot4, had a lower viral titer pretreatment on day 8 than on day 5, suggesting that the animal may have been recovering from infection naturally.

Animals that received hu199 had no detectable virus by plaque assay at any of the remaining test points (*SI Appendix, Fig. S1B*). None of the four animals displayed any substantial signs of illness or had clinical scores throughout the experiment. On necropsy at 35 dpi, plaque titration of spleen, liver, and brain (frontal lobe and brainstem) homogenates yielded no detectable virus. Furthermore, histopathology was performed on an extensive set of tissues, and no evidence of viral antigen was detected by immunohistochemistry (IHC) analysis in any tissue of the treated animals (*SI Appendix, Table S2*), whereas antigen was detected in almost all tissues of the two historical controls infected with the Romero strain (animals HCR1 and HCR2). Although only very limited conclusions can be drawn from this pilot experiment lacking an internal control, these results provided guidance for the design of a more robust follow-up experiment in NHPs.

Based on the results from the pilot study and clinical preference for a single-dose therapeutic, we next tested the efficacy of a single treatment provided at either 6 or 8 dpi in an attempt to frame the therapeutic window. Groups of cynomolgus macaques were inoculated intramuscularly (i.m.) with 5,000 PFU of either the Espindola or the Romero strain of JUNV. NHPs were treated with a single i.v. dose of hu199 (50 mg/kg) at 6 or 8 dpi. The control inoculated with Espindola (CE) succumbed to disease at 15 dpi (MTD including two historical controls,  $17 \pm 4$  d; Fig. 2 and *SI Appendix, Table S3*), while the control inoculated with Romero (CR) succumbed at 22 dpi (MTD including historical controls,  $19 \pm 5$  d; Fig. 2 and *SI Appendix, Table S4*). In contrast, all NHPs treated with hu199 experienced a significant survival benefit ( $P < 0.05$ , log-rank test) compared to controls, with 100% of animals challenged with Espindola and treated at 6 dpi ( $n = 4$ ) surviving to the study endpoint at 35 dpi. In both the Espindola and Romero challenge models, mAb treatment at 8 dpi afforded protection to 50% of the animals. Not unexpectedly, severe weight loss was associated with mortality; 5 of the 6 NHPs that succumbed in this experiment experienced weight loss of  $>15\%$  (Fig. 2). Some animals experienced transient fever ( $\geq 1.5^\circ\text{C}$ ) between 6 and 15 dpi, but fever was not predictive of outcome (*SI Appendix, Tables S3 and S4*).

All animals were viremic on the day of treatment by both plaque and RT-PCR assays, performed on plasma and whole blood, respectively (Fig. 2). By plaque assay, the four Espindola-inoculated animals treated at 6 dpi had a mean viral load of  $2.7 \pm 0.7 \log_{10}$  PFU/mL prior to dosing with hu199. In the animals treated at 8 dpi, mean viral loads of  $3.2 \pm 0.7 \log_{10}$  PFU/mL (Espindola) and  $2.5 \pm 0.4 \log_{10}$  PFU/mL (Romero) were observed prior to mAb dosing. RT-PCR assay revealed a mean viral load of  $6.7 \pm 1.2 \log_{10}$  copies/mL in the four Espindola-infected animals treated at 6 dpi,  $8.4 \pm 0.2 \log_{10}$  copies/mL in the four Espindola-infected animals treated at 8 dpi, and  $7.8 \pm 0.4 \log_{10}$  copies/mL in the four Romero-infected animals treated at 8 dpi. Therapeutic administration of hu199 resulted in a dramatic reduction in viral load in the plasma as assessed by plaque assay in all animals, with levels of infectious virus in all treated animals below the limit of detection at the first sampling time point after dosing. Viral load, as assessed by RT-PCR of whole blood, was modestly reduced in most animals after treatment with hu199 but was detected throughout the study.

Given the absence of infectious virus detected in any survivor after 11 dpi, and because the RT-PCR assay was performed on whole blood, we speculated that the RT-PCR signal detected toward the end of the study was due to degraded viral genetic material, either adhering to cells or that had been phagocytosed. To test this hypothesis, RT-PCR was run on plasma obtained from all surviving animals at 35 dpi to specifically identify genetic material that would be present in circulating virions. Seven of eight animals were negative by this assay, suggesting that the genetic material detected in the majority of animals by RT-PCR of whole blood at 35 dpi (Fig. 2) was cell-associated. The presence

of an RT-PCR signal in the plasma of the one outlier, NHP 7, but with the absence of any detected infectious virus by plaque assay (Fig. 2) is difficult to explain. It is noteworthy that NHP 7 had the highest viral titer by plaque assay of any of the Espindola-inoculated animals prior to treatment with hu199. The positive RT-PCR signal may have been due to a contamination event, ongoing clearance of residual vRNA after resolution of infection, detection of virus bound and neutralized by circulating antibody, or potential detection of shedding of viral genetic material from an immune-privileged site other than the brain, a site in which no infectious virus was detected (Table 1).

The results of plaque assays performed on selected tissues on necropsy are presented in Table 1. While control animals (CE and CR) had infectious virus present in liver, spleen, and brain tissue, no infectious virus was detected in these tissues from treated survivors, with the exception of one of the animals treated at 8 dpi (NHP 8), in which virus was detected in the brainstem. Also noteworthy is the absence of virus detected in liver tissue of NHP 5, which succumbed very late in the study (34 dpi). This animal also did not have virus detected in blood by plaque assay after 8 dpi.

Clinically, all contemporaneous (CE and CR) and historical (HCE1, HCE2, HCR1, and HCR2) control animals displayed evidence of neurologic symptoms, including ataxia (one of three Romero-inoculated), myoclonus (one of three Espindola-inoculated), intention tremors (two of three Espindola-inoculated and one of three Romero-inoculated), and seizures (two of three Espindola-inoculated and one of three Romero-inoculated) (Fig. 3 and *SI Appendix, Tables S3 and S4*). Animals also experienced facial edema (one of three for both groups), petechial rash (two of three for both groups), and diarrhea (one of three Espindola-inoculated and two of three Romero-inoculated). In marked contrast, animals treated with hu199 at 6 dpi displayed minimal signs of illness, with reduced appetite (biscuit consumption; three of four) the sole observation. The surviving animals treated at 8 dpi also experienced minimal symptoms, with reduced appetite in one of two Espindola-inoculated survivors and two of two Romero-inoculated survivors and diarrhea in one Espindola-inoculated survivor.

Various changes in clinical pathology were noted before and after hu199 treatment of all JUNV-infected macaques, including lymphocytopenia, granulocytopenia, monocytopenia, thrombocytopenia, anemia, hypoalbuminemia, elevations in liver-associated enzymes (aspartate aminotransferase and alanine aminotransferase), and/or elevations in C-reactive protein (*SI Appendix, Tables S3 and S4*). These changes were mostly transient and returned to normal values in all macaques that survived to the study endpoint.

IHC analysis performed on tissues from necropsy revealed diffuse staining, indicating the presence of JUNV antigen, in almost all tissues of the Espindola and Romero contemporaneous and historical controls (*SI Appendix, Table S5 and Fig. S2*). In contrast, no antigen was detected in any tissue of two of the Espindola-inoculated NHPs treated at 6 dpi (NHPs 1 and 4; *SI Appendix, Table S2*). NHP 2 and 3 from this group had multifocal clusters of staining in multiple regions of the brain (brainstem and hippocampus regions). One of the two surviving Espindola-inoculated animals, NHP 7, treated at 8 dpi had multifocal clustered staining in the hippocampus region of the brain and eye, while the other, NHP 8, had diffuse antigen detected in the brain and eye. The two treated Espindola-inoculated animals that succumbed to AHF (NHP 5 and 6) had antigen detected in the majority of tested tissues, similar to the untreated controls. Similar observations were observed in the treated Romero-inoculated animals (*SI Appendix, Fig. S3*), with treated survivors having staining limited to the brain (NHP 9) or the cervical spinal cord and eye (NHP 12) and animals that succumbed (NHP 10 and 11) showing staining patterns similar to those seen in controls.

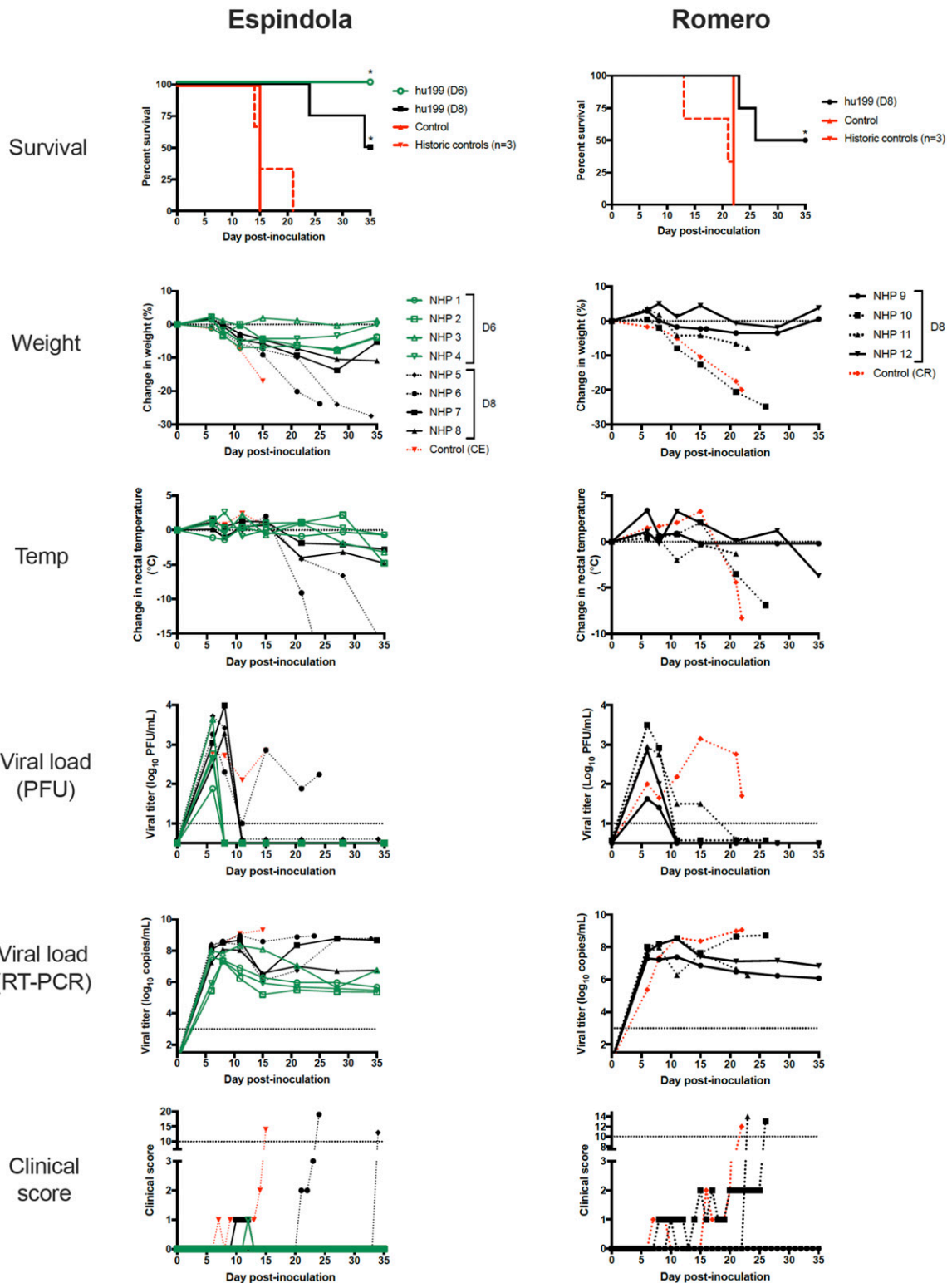


**Fig. 2.** Therapeutic efficacy of hu199 in NHPs inoculated with JUNV (Espindola, left column; Romero, right column). Survival: NHPs were inoculated with 5000 PFU of Romero or 5000 PFU of Espindola. NHPs were treated with hu199 (50 mg/kg) at either 6 dpi (D6) or 8 dpi (D8). Survival was significantly better in the treated groups than in the historical controls ( $P < 0.05$ ). Weight, temperature, viral load, and clinical score figures: Data from animals that succumbed to disease are represented by dashed lines. The horizontal dashed lines represent baseline weight and temperature (weight and temperature figures), the limit of detection for the assay (viral load figures), or the clinical score that triggers euthanasia according to the IACUC-approved protocol (clinical score figures).



**Table 1. Viral load in selected tissues on necropsy**

NHP	Virus	Treatment	Outcome	dpi of death/necropsy	Viral titer (log <sub>10</sub> PFU/g)			
					Liver	Spleen	Brain (frontal)	Brain (stem)
1	Espindola	D6	Survived	35	0	0	0	0
2	Espindola	D6	Survived	35	0	0	0	0
3	Espindola	D6	Survived	35	0	0	0	0
4	Espindola	D6	Survived	35	0	0	0	0
5	Espindola	D8	Died	34	0	3.1	5.1	5.7
6	Espindola	D8	Died	24	4.6	4.5	NT	NT
7	Espindola	D8	Survived	35	0	0	0	0
8	Espindola	D8	Survived	35	0	0	0	3.0
CE	Espindola	In-study control	Died	15	3.9	4.1	2.9	3.4
HCE1	Espindola	Historical control	Died	21	6.3	4.5	5.8	6.0
HCE2	Espindola	Historical control	Died	14	7.5	5.3	3.9	3.9
9	Romero	D8	Survived	35	0	0	0	0
10	Romero	D8	Died	26	3.1	3.5	NT	NT
11	Romero	D8	Died	23	2.9	2.7	NT	NT
12	Romero	D8	Survived	35	0	0	0	0
CR	Romero	In-study control	Died	22	3.7	3.8	6.4	5.8
HCR1	Romero	Historical control	Died	13	8.0	7.5	5.3	5.3
HCR2	Romero	Historical control	Died	21	6.9	6.2	5.5	4.9

NT, not tested.

**Discussion**

The pathogenesis observed in the untreated control macaques was consistent with most previous reports of AHF in NHPs, despite the fact that previous studies used rhesus macaques and an i.m. inoculation route instead of the cynomolgus macaques and i.v. route used in the present study (15–18). However, in the one previous NHP study performed with Romero, only mild transient disease with no mortality was observed (17), a distinct contrast from the severe and lethal illness observed in our study. That study differed from the present study in the route of

inoculation (i.m.) and the use of rhesus macaques. Although clinical differences between Espindola and Ledesma strains have been reported in NHPs (15, 18), no significant differences were observed between the small numbers of control animals inoculated with Espindola or Romero in the present study. Both strains resulted in a combination of hemorrhagic and neurologic symptoms consistent with AHF observed in human patients.

In marked contrast, when Romero-inoculated animals in the pilot study and Espindola-inoculated animals in the main study were treated with hu199 at 5 and 6 dpi, respectively (time points

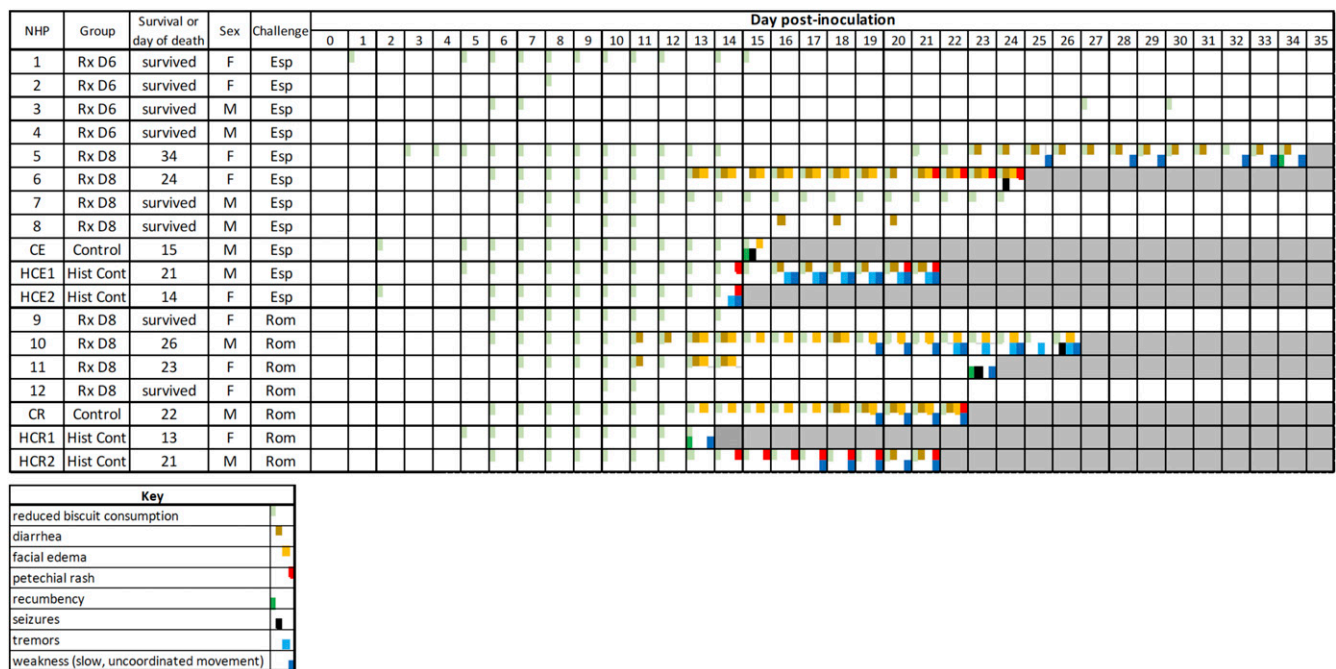


**Fig. 3.** Clinical observations of JUNV-inoculated NHPs. Note that these observations do not include all factors used in determining the clinical score depicted in Fig. 2. Solid gray boxes indicate that no observations were obtained because the animal had previously succumbed to infection. Rx, treatment group; Esp, Espindola; Rom, Romero; HCE, historical control inoculated with Espindola; HCR, historical control inoculated with Romero.

when all animals were viremic), clinical symptomology was either completely absent or minimal. No infectious virus was detectable in the blood of these animals at the next sampling time point. Delaying hu199 treatment to 8 dpi resulted in a decrease in survival to 50%. IHC analysis performed on tissues obtained at necropsy from animals that survived the 35 d of the study period detected viral antigen in one-half of the animals treated with hu199 at 6 dpi and in all animals treated at 8 dpi. JUNV antigen was observed only in tissues from immune-privileged sites (brain and eye). In contrast, controls and treated animals that succumbed to AHF had evidence of viral antigen in almost all tissues tested, indicating disseminated and poorly controlled infection. Whether detection of viral antigen by IHC in animals surviving the 35 d study period is indicative of an active infection that would have progressed to AHF and death given more time or of a latent infection akin to the late neurologic syndrome (LNS) observed in some human survivors of AHF (15) is unknown. This question, as well as the late death of NHP 5 and the detection of live virus by plaque assay in the brainstem on necropsy of surviving NHP 8, suggest that ideally, animals should be observed longer in AHF studies, when BSL-4 space and budget limitations allow.

Our findings in cynomolgus macaques are consistent with clinical reports of patients treated with immune plasma, although the treatment window is longer in humans; treatment within 8 d after appearance of initial symptoms (as opposed to 5 to 8 d after exposure in NHPs) is generally successful (9). This difference may be due to differences in the viral exposure/challenge dose and routes of infection; human infection is transmitted primarily across mucosal surfaces, while the cynomolgus macaque AHF model described here uses an i.v. challenge. In humans who survive AHF, neurologic involvement (i.e., LNS) is observed in ~10% of patients treated with immune plasma but has only been reported rarely in patients who recovered without antibody treatment (15). Rather than immune plasma playing a direct role in spread of virus across the blood-brain barrier (BBB), we speculate that this observed increase is due to immune plasma treatment rescuing patients at a stage in the disease where the BBB has been breached and who otherwise would have succumbed from systemic infection without treatment. Although some circulating antibody can be found in cerebrospinal fluid, this is generally at 0.1% to 0.01% of the concentration in circulation (19, 20), which likely explains the inability of antibody treatment to rescue patients after 8 d of initial symptoms. Supplementing antibody treatment with an antiviral agent capable of crossing the BBB may be worth exploring to expand the therapeutic window for AHF treatment.

In guinea pigs, a variety of nonantibody experimental therapeutics have been evaluated (12), including ribavirin and favipiravir (T-705). Although some survival benefit was observed when these agents were administered soon after inoculation, none was as efficacious as immune plasma and mAbs, which provided 100% protection when delivered as late as 6 dpi (12, 21). Ribavirin has also been evaluated in a macaque model of AHF. Initiation of treatment at 30 min after inoculation resulted in four of four NHPs surviving, while treatment initiated at 6 dpi resulted in one of four surviving, with a delay to death observed in two of the animals (16). There is some evidence of an antiviral effect with ribavirin, a drug that does not cross the BBB, in human AHF patients, but no apparent benefit after the 8-d window after onset of symptoms (22).

The data presented here suggest that mAbs could be an efficacious replacement for immune plasma in AHF therapy. We previously estimated the cost of an adult human dose of the cJ199 mAb as under \$200 (12). Thus, mAb therapy for AHF appears to be technically and economically feasible. However, it is not the manufacturing costs that present a hurdle to the clinical use of mAbs for rare diseases like AHF, but rather the expenses—conservatively estimated as several hundred million dollars—

associated with developing a biologic through licensure (e.g., via the Food and Drug Administration or European Medicines Agency). For rare, endemic viral diseases with high morbidity and mortality but with commercial markets that are unable to justify the expense of bringing a drug to licensure, it may be sensible and cost-efficient to enable small-scale local manufacturing of mAbs specific for the diseases impacting the local population, working with local regulators where possible, to use the drug(s) under expanded access and/or other local compassionate use provisions, ideally after performance of a Phase 1 safety study. mAb production is a rather straightforward and routine laboratory practice; mAbs made even in academic laboratory settings have been utilized in clinical settings for compassionate use (23).

## Materials and Methods

**Humanization of J199.** Humanization of J199 (murine mAb GB-03-BE08) (11) focused on murine framework domains that demonstrated >85% identity with the human germ line. Sequences were also analyzed for hot spots (e.g., free cysteines, Fv N-linked glycosylation sites, covariance violations, deamidation sites, isomerization sites, CDR3 tryptophan oxidation sites) and hydrophobic surface patches. All analyses were done using Molecular Operating Environment software (Chemical Computing Group). Framework/CDR junctions were inspected and rarely altered (13). Humanized VRs were designed using human framework substitutions when those substitutions were found in >75% of germ line matches. Ten humanized VH sequences and two humanized VL sequences were synthesized, cloned into expression vectors, and expressed in *N. benthamiana* using the Magnicon system (24). Approximately 70 unique antibody combinations involving different vector backbones, signal peptides, and the humanized VH and VL sequences were tested for expression level and antigen binding, and one combination was selected based on adequate expression level, antigen binding, and viral neutralization activity.

To generate an mAb supply for the guinea pig study, genes containing the variable region sequences were synthesized (Life Technologies) and subsequently cloned into the Magnicon plant expression vectors (TMV and PVX; Icon Genetics) containing codon-optimized human kappa and human IgG<sub>1</sub> constant regions, followed by transformation into *Agrobacterium tumefaciens* strain ICF320 (Icon Genetics). *N. benthamiana* plants genetically modified to produce highly homogenous mammalian N-glycans of the GnG glycoform (25) were grown for 4 wk in an enclosed growth room (20 to 23 °C) and used for vacuum infiltration as described previously (26). At 7 d postinfiltration, the mAb was extracted from the leaf tissue and purified via protein A chromatography (26), then passed through an Acrodisc unit with Mustang Q Membrane (Pall Life Sciences) using a syringe for endotoxin reduction. Endotoxin levels were measured with Endosafe PTS (Charles River) and were <100 EU/mg.

**Production of hu199 for NHP Efficacy Studies.** Hu199 mAb was expressed using a nonfucosylated CHOK1-AF host cell line. Stable pools were generated by chemical transfection of the CHOK1-AF host with a bicistronic vector (ATUM) containing a GS selection marker and the mAb heavy and light chains. Stable pools were selected with methionine sulfoximine and enriched using a ClonePix2 colony picker (Molecular Devices). ClonePix nonclonal isolates were grown and expanded in static culture, followed by suspension culture in shake flasks. Clonal cell lines were derived from the top isolate by limiting the dilution and subsequent verification of monoclonality using a CloneSelect imager (Molecular Devices). Production of hu199 mAb for in vivo studies was carried out using a clonal cell line. Cells were grown in 5-L shake flasks in fed batch culture using BalanCD CHO Growth A (Fujifilm Irvine Scientific) and CHO Feed 4 (Fujifilm Irvine Scientific) in a humidified shaker incubator (Kuhner) at 36.5 °C and 140 rpm with 5% CO<sub>2</sub>. After 14 d in fed batch culture, the supernatants were collected and filtered using Rapid Clear Cap assembly (Thomson Instrument). Filtered supernatants were stored at 4 °C until mAb purification. The conditioned medium was loaded onto a Mab-Select SuRe LX Protein A column (Cytiva), washed with PBS, and then eluted using 0.1 M acetic acid containing 0.2 M L-arginine, pH ~3.0. The resulting eluate was neutralized with 2 M Tris base to pH ~7.0.

The mAb was further polished using a Capto Q column (Cytiva) in a passive mode to help remove host cell protein and DNA. In brief, the neutralized post-protein A eluate was diluted five-fold using water for injection to reduce the conductivity to ≤6 mS/cm, and the pH was adjusted to ~7.5 before loading onto the Capto Q column. The diluted sample was loaded and washed with 50 mM Hepes, pH 7.0. The flowthrough and the wash

containing the hu199 mAb were collected and subjected to tangential flow filtration (TFF) and buffer-exchanged into formulation buffer (20 mM citrate, 10 mM glycine, 8% sucrose, pH 5.5). Polysorbate-80 was added to 0.01% after the completion of TFF. The concentration of the formulated drug substance was 22.7 mg/mL with 99.7% monomer via size exclusion high-performance liquid chromatography and an endotoxin level of 0.05 EU/mg.

**Plaque Reduction Neutralization Assay.** The mAbs were serially diluted threefold in infection medium (MEM supplemented with 1% FBS, L-glutamine, and pen/strep) starting at 200 µg/mL. JUNV virus strain Candid #1 was diluted in infection medium to 2,000 PFU/mL. Each dilution of the antibodies was mixed with an equal volume of virus to achieve a final concentration of 100 µg/mL and 100 PFU. A virus-only control was incubated with medium alone. The dilutions were then incubated for 1 h at 37 °C in a humidified CO<sub>2</sub> atmosphere. Vero cells seeded in 24-well plates to near confluency were infected with the dilutions for 1 h before 0.8% methylcellulose was added as an overlay. After 8 d, plaques were visualized by staining the cell monolayer with crystal violet in 5% glutaraldehyde.

**Animal Studies.** Guinea pig and NHP studies were completed under BSL-4 biocontainment at the Galveston National Lab and were approved by the University of Texas Medical Branch (UTMB) Institutional Laboratory Animal Care and Use Committee (IACUC). The UTMB facilities used in this work are accredited by the Association for Assessment and Accreditation of Laboratory Animal Care International and adhere to principles specified in the eighth edition of the National Research Council's *Guide for the Care and Use of Laboratory Animals*.

**Guinea Pig Model.** The guinea pig model for JUNV strain Romero (P3235) has been described previously (12). In brief, female outbred Hartley guinea pigs (351 to 400 g) were purchased from Charles River Laboratories and subsequently quarantined and acclimatized for 2 to 7 d prior to challenge. Transponders for temperature recording were implanted before the acclimatization period. Individual animals were infected with ~1,000 PFU by i.p. injection. *N. benthamiana*-derived mAbs were administered i.p. in volumes of 0.8 to 0.9 mL. Studies were concluded at 35 dpi. Survival curves were analyzed with the log-rank (Mantel-Cox) test using GraphPad Prism version 7.0e. All studies were performed with the same stock of virus, using the same protocols, and by the same personnel.

**NHP Efficacy Testing.** Twenty-two healthy JUNV-naive (~3 to 5 kg, age 3 to 6 y) cynomolgus macaques (*Macaca fascicularis*; PreLabs) were used for these studies. The initial studies used four macaques to assess the lethality of the JUNV seed stocks: Romero P3235 (GenBank accession nos. MW227338 and MW227339) and Espindola P3790 (GenBank accession nos. MW227336 and MW22737), kindly provided by Thomas Ksiazek. Although previous studies focused on i.m. inoculation, we opted for i.v. delivery of the viral challenge. Human exposure is believed to occur on mucosal surfaces; viral entry through mucosa would be more likely to result in virus in the blood than in muscle tissue. In brief, two macaques were exposed to a target dose of 5,000 PFU of the Romero strain by i.v. injection, and two macaques were exposed to a target dose of 5,000 PFU of the Espindola strain by i.v. injection. Then a pilot study was performed to assess the protective efficacy of hu199. Four macaques were exposed to a target dose of 5,000 PFU of the Romero strain; one animal was treated i.v. with a single dose of hu199 (50 mg/kg) on day 5 after virus exposure, and two animals were treated i.v. on days 5 and 8 after exposure with hu199 (50 mg/kg/dose).

Based on the success of the pilot study, a larger study was conducted to more fully assess the efficacy of hu199 against both the Romero and Espindola strains. In this study, 14 macaques were randomized into three treatment groups of four animals each and two control groups of one animal each. All 14 animals were exposed to a target dose of 5,000 PFU i.v. of either the Romero strain ( $n = 5$ ) or the Espindola strain ( $n = 9$ ). One group of macaques ( $n = 4$ ) received a single dose of hu199 (50 mg/kg) i.v. on day 6 after the Espindola strain challenge, another group of macaques ( $n = 4$ ) received a single dose of hu199 i.v. on day 8 after the Romero strain challenge, and a third group of animals received a single dose of hu199 i.v. on day 8 after the Espindola challenge. The two control animals (one Romero and one Espindola) were not treated. The use of individual controls and comparisons with historical controls using the same viral stock and protocols performed by the same personnel has become routine in many high-containment laboratories for highly lethal pathogens and is preferred by many IACUCs. The decision for this study was dictated by budgetary constraints, BSL-4 space limitations, and the UTMB IACUC.

The macaques were monitored daily and scored for disease progression with an internal AHF humane endpoint scoring sheet approved by the UTMB IACUC. The scoring changes measured from baseline included posture and activity level, attitude and behavior, food intake, respiration, and disease manifestations, such as visible rash, hemorrhage, ecchymosis, or flushed skin, as well as central nervous system abnormalities. A score of  $\geq 10$  indicated that the animal met the criteria for euthanasia. All studies were performed with the same stock of virus, using the same protocols, and by the same personnel.

**Plaque Assay.** Serial 10-fold dilutions of either plasma samples or 10% clarified tissue homogenates were adsorbed to Vero E6 monolayers in duplicate wells of six-well plates (200 µL/well). Following adsorption, the inoculum was removed by aspiration, and the monolayers were overlaid with 3 mL of 0.8% SeaPlaque agarose in DMEM. The agarose was permitted to set at room temperature for 15 min, and the plates were then incubated at 32 °C under 5% CO<sub>2</sub> for 4 to 5 d to allow plaque development. The limit of detection was 5 PFU/mL for plasma samples and 250 PFU/g for tissue samples.

**RT-PCR Assay.** RNA was isolated from whole blood using the viral RNA Mini Kit (Qiagen) using 100 µL of blood into 600 µL of viral lysis buffer AVL. The primers and probe targeting the GPC gene of JUNV were used for RT-qPCR; the Romero probe was 6-carboxyfluorescein (6FAM)-5' TGA CGC TGT GAA GAA TAC TGT GCT CC 3'-carboxytetramethylrhodamine (TAMRA) (Life Technologies), while the Espindola probe was 6FAM-5' CGC CAA CTC CAT CAG TTC ATC CCT 3'-TAMRA. JUNV RNA was detected using the Bio-Rad CFX96 detection system and the Qiagen OneStep probe RT-qPCR kit with the following cycle conditions: 50 °C for 10 min, 95 °C for 10 s, and 40 cycles of 95 °C for 10 s and 55.7 °C for 30 s. Threshold cycle values representing JUNV S genomes were analyzed with CFX Manager software, and data are shown as genome equivalents (GEq). To create the GEq standard, RNA from JUNV stocks was extracted, and the number of JUNV S genomes was calculated using Avogadro's number, the molecular weight of the JUNV genome, and the percentage of the S genome segment to total viral RNA genomes present in the standard sample. The limit of detection was  $1 \times 10^3$  GEq/mL.

**Hematology and Serum Biochemistry.** Total white blood cell counts, white blood cell differentials, red blood cell counts, platelet counts, hematocrit values, total hemoglobin concentrations, mean cell volumes, mean corpuscular volumes, and mean corpuscular hemoglobin concentrations were analyzed from blood collected in EDTA-containing tubes using a laser-based hematologic analyzer (Beckman Coulter). Serum samples were tested for concentrations of alanine aminotransferase, albumin, alkaline phosphatase, amylase, aspartate aminotransferase, C-reactive protein, calcium, creatinine, gamma-glutamyltransferase, glucose, total protein, blood urea nitrogen, and uric acid using a Piccolo point-of-care analyzer and Biochemistry Panel Plus analyzer discs (Abaxis).

**Histopathology and Immunohistochemistry.** Necropsy was performed on all animals, and representative tissue samples were collected. The tissues were stored for at least 21 d in 10% neutral buffered formalin in the BSL-4, and the formalin was changed prior to removal from the BSL-4. Formalin-fixed tissues were then processed in the BSL-2 and embedded in paraffin wax. Embedded tissue blocks were sectioned at 4 µm and dried at 60 °C. The sections were deparaffinized and rehydrated in xylene, graded ethanol, and deionized water. Antigen retrieval incubation was performed in a 10 mM, pH 6 citrate buffer for 20 min at 95 °C, then allowed to cool at room temperature for 20 min. The sections were then quenched in a solution of 3% hydrogen peroxide for 10 min before being processed for IHC analysis using the Thermo Scientific Lab Vision Autostainer 360. Avidin D and biotin (Vector Laboratories; SP-2001) were then applied for 15 min to block endogenous biotin reactivity. Specific anti-JUNV immunoreactivity was detected using an anti-JUNV primary antibody at 1:1,000 dilution for 1 h (LifeSpan Bio; LS-C500445). The secondary antibody used was biotinylated goat anti-rabbit IgG (Vector Laboratories; BA-1000) at 1:200 for 30 min, followed by streptavidin-HRP (Vector Laboratories; SA-5704) for 30 min. Slides were developed with DAB chromagen (Dako; K3468) for 5 min and then counterstained with hematoxylin for 1 min.

**Data Availability.** Anti-JUNV mAbs can be obtained through a material transfer agreement with Mapp Biopharmaceutical.

**ACKNOWLEDGMENTS.** We thank Daniel Deer, Dr. Chad Mire, and Dr. Kevin Melody for assistance with animal studies; Natalie Dobias for assistance with

tissue preparation and IHC analysis; and the UTMB Animal Resource Center for animal husbandry support. This publication was made possible by National Institute of Allergy and Infectious Disease (NIAID) Grants AI111391 and

AI142777. Its contents are solely the responsibility of the authors and do not necessarily represent the official views of the NIAID, NIH, or UTMB at Galveston.

1. C. J. Peters, Emerging infections: Lessons from the viral hemorrhagic fevers. *Trans. Am. Clin. Climatol. Assoc.* **117**, 189–196, discussion 196–197 (2006).
2. R. H. Kenyon *et al.*, Aerosol infection of rhesus macaques with Junin virus. *Intervirology* **33**, 23–31 (1992).
3. M. J. Buchmeier, C. J. Peters, "Arenaviridae: The viruses and their replication." in *Fields Virology*, D. M. Knipe, P. M. Howley, Eds. (Lippincott Williams & Wilkins, 2007), pp. 1791–1827.
4. A. Grant *et al.*, Junin virus pathogenesis and virus replication. *Viruses* **4**, 2317–2339 (2012).
5. M. C. Weissenbacher, L. B. de Guerrero, M. C. Boxaca, Experimental biology and pathogenesis of Junin virus infection in animals and man. *Bull. World Health Organ.* **52**, 507–515 (1975).
6. J. I. Maiztegui *et al.*, AHF Study Group, Protective efficacy of a live attenuated vaccine against Argentine hemorrhagic fever. *J. Infect. Dis.* **177**, 277–283 (1998).
7. D. A. Enria, A. M. Ambrosio, A. M. Briggiler, M. R. Feuillade, E. Crivelli; Study Group on Argentine Hemorrhagic Fever Vaccine, [Candid #1 vaccine against Argentine hemorrhagic fever produced in Argentina: Immunogenicity and safety] [in Spanish]. *Medicina (B. Aires)* **70**, 215–222 (2010).
8. D. A. Enria, A. M. Briggiler, N. J. Fernandez, S. C. Levis, J. I. Maiztegui, Importance of dose of neutralising antibodies in treatment of Argentine haemorrhagic fever with immune plasma. *Lancet* **2**, 255–256 (1984).
9. D. A. Enria, A. M. Briggiler, Z. Sánchez, Treatment of Argentine hemorrhagic fever. *Antiviral Res.* **78**, 132–139 (2008).
10. D. A. Enria, J. I. Maiztegui, Antiviral treatment of Argentine hemorrhagic fever. *Antiviral Res.* **23**, 23–31 (1994).
11. A. Sanchez *et al.*, Junin virus monoclonal antibodies: Characterization and cross-reactivity with other arenaviruses. *J. Gen. Virol.* **70**, 1125–1132 (1989).
12. L. Zeitlin *et al.*, Monoclonal antibody therapy for Junin virus infection. *Proc. Natl. Acad. Sci. U.S.A.* **113**, 4458–4463 (2016).
13. J. W. Stave, K. Lindpaintner, Antibody and antigen contact residues define epitope and paratope size and structure. *J. Immunol.* **191**, 1428–1435 (2013).
14. L. Zeitlin *et al.*, Enhanced potency of a fucose-free monoclonal antibody being developed as an Ebola virus immunoprotectant. *Proc. Natl. Acad. Sci. U.S.A.* **108**, 20690–20694 (2011).
15. D. E. Green, B. G. Mahlandt, K. T. McKee Jr, Experimental Argentine hemorrhagic fever in rhesus macaques: Virus-specific variations in pathology. *J. Med. Virol.* **22**, 113–133 (1987).
16. K. T. McKee Jr, J. W. Huggins, C. J. Trahan, B. G. Mahlandt, Ribavirin prophylaxis and therapy for experimental Argentine hemorrhagic fever. *Antimicrob. Agents Chemother.* **32**, 1304–1309 (1988).
17. K. T. McKee Jr, B. G. Mahlandt, J. I. Maiztegui, G. A. Eddy, C. J. Peters, Experimental Argentine hemorrhagic fever in rhesus macaques: Viral strain-dependent clinical response. *J. Infect. Dis.* **152**, 218–221 (1985).
18. K. T. McKee Jr, B. G. Mahlandt, J. I. Maiztegui, D. E. Green, C. J. Peters, Virus-specific factors in experimental Argentine hemorrhagic fever in rhesus macaques. *J. Med. Virol.* **22**, 99–111 (1987).
19. H. Reiber, Dynamics of brain-derived proteins in cerebrospinal fluid. *Clin. Chim. Acta* **310**, 173–186 (2001).
20. M. Tabrizi, G. G. Bornstein, H. Suria, Biodistribution mechanisms of therapeutic monoclonal antibodies in health and disease. *AAPS J.* **12**, 33–43 (2010).
21. R. H. Kenyon, D. E. Green, G. A. Eddy, C. J. Peters, Treatment of junin virus-infected Guinea pigs with immune serum: Development of late neurological disease. *J. Med. Virol.* **20**, 207–218 (1986).
22. D. A. Enria *et al.*, Tolerance and antiviral effect of ribavirin in patients with Argentine hemorrhagic fever. *Antiviral Res.* **7**, 353–359 (1987).
23. E. G. Playford *et al.*, Safety, tolerability, pharmacokinetics, and immunogenicity of a human monoclonal antibody targeting the G glycoprotein of henipaviruses in healthy adults: A first-in-human, randomised, controlled, phase 1 study. *Lancet Infect. Dis.* **20**, 445–454 (2020).
24. A. Giritich *et al.*, Rapid high-yield expression of full-size IgG antibodies in plants co-infected with noncompeting viral vectors. *Proc. Natl. Acad. Sci. U.S.A.* **103**, 14701–14706 (2006).
25. R. Strasser *et al.*, Generation of glyco-engineered *Nicotiana benthamiana* for the production of monoclonal antibodies with a homogeneous human-like N-glycan structure. *Plant Biotechnol. J.* **6**, 392–402 (2008).
26. L. Zeitlin *et al.*, Prophylactic and therapeutic testing of *Nicotiana*-derived RSV-neutralizing human monoclonal antibodies in the cotton rat model. *MAbs* **5**, 263–269 (2013).